# Thermal coupling within LTP dynamics control loop

Journal of Physics: Conference Series **154** (2009) 012004 doi:10.1088/1742-6596/154/1/012004

# Thermal coupling within LTP dynamics control loop

**M Nofrarias[1], AF García Marín[1], G Heinzel[1], M Hewitson[1], A Lobo[2,3], J Sanjuán[2,3], J Ramos-Castro[4], K Danzmann[1]**

[1] Max-Planck-Institut für Gravitationsphysik, Albert Einstein Institut (AEI), Callinstrasse 38, 30167 Hannover, Germany
[2] Institut de Ciències de l'Espai (ICE-CSIC), Facultat de Ciències , Torre C5, 08193 Bellaterra, Spain
[3] Institut d'Estudis Espacials de Catalunya (IEEC), Edifici Nexus, Gran Capità 2-4, 08034 Barcelona, Spain
[4] Departament d'Enginyeria Electrònica, UPC, Campus Nord, Edifici C4, Jordi Girona 1-3, 08034 Barcelona, Spain

E-mail: miquel.nofrarias@aei.mpg.de

**Abstract.** The Diagnostic Subsytem in the LISA Technology Package (LTP) on board the LISA Pathfinder mission (LPF) will characterise those external disturbances with a potential impact on the performance of the experiment coming from either thermal, magnetic or charged particles perturbations. A correct design of the experiments to measure these effects in flight requires a closed loop analysis that takes into account the dynamics of the test masses, the force applied by the controllers and those noisy terms (coming from sensing or force noise) that enters into the loop. We describe this analysis in the thermal case and we give a first numerical example of the instrument response to controlled thermal inputs.

## 1. Introduction

The LISA Technology Package Experiment (LTP) [1] on board LISA Pathfinder (LPF) mission will test key technologies for the future space borne gravitational wave detector LISA [2], a collaborative project between ESA and NASA. The LTP main concept consists in two test masses in nominally geodesic motion inside two separate high vacuum chambers; an optical metrology subsystem (OMS) [3] senses the relative distance to a given level of resolution that fixes the instrumental sensitivity. The test mass position relative to the spacecraft is controlled by the surrounding electrodes which act both as sensing and actuator elements; jointly with the micropopulsion thrusters they conform the Gravitational Reference Sensor (GRS) [4]. The high gain drag-free control loop forces the spacecraft to follow one test mass whereas the low frequency suspension loop allows to keep the differential acceleration noise between both test masses in the required top level performance sensitivity. For the LPF this value is expressed as

$$\mathrm{S}_{\Delta\mathrm{a}}^{1/2}(\omega) \leq 3\times 10^{-14}\left[1+\left(\frac{\omega/2\pi}{3\,\mathrm{mHz}}\right)^2\right]\,\mathrm{m\,s^2/\sqrt{Hz}} \qquad (1)$$

in the bandwidth $1\,\mathrm{mHz} \leq \omega/2\pi \leq 30\,\mathrm{mHz}$. There are various noise sources contributing to this noise budget and, among these, there are some that will be monitored by the Diagnostic Subsystem of the LTP [5], which is designed to measure temperature and magnetic fluctuations

in those places where these magnitudes have a particular strong coupling with the main geodesic measurement, and that also will characterise the charged particle shower hitting the test mass. Diagnostics will play an active role as well in the noise model investigation process during the mission lifetime. The temperature and magnetic subsystem will count with heaters and coils which will allow, not only an environmental characterisation, but a full noise projection campaign. In particular, we will address here the thermal diagnostic case, consisting on 24 NTC (Negative Temperature Coefficient) sensors, 14 heaters and the front-end electronics [6] already tested to achieve the required performance [7]. Although on ground characterisation of these environmental coupling have been already performed, the experiment design on board the satellite needs to take into account the in-loop operation of the mission. In the following we will briefly describe how thermal experiments enter into the LTP control loop and give some numerical examples of the kind of signals planned to be injected. Before that, we first summarise the experimental results of some thermal coupling factors obtained so far.

## 2. Open loop characterisation of thermal effects

Thermal experiments on board the LTP can be split in three different groups: (1) experiments on the Electrode Housing (EH), (2) experiments on the Optical Window (OW) and (3) experiments on the CFRP (Carbon Fiber Reinforced Plastic) struts holding the LTP Core Assembly inside the thermal shield. Among these, experimental results exist for the two first ones and those will be the ones addressed here. The third one is more of a structural kind and has been studied by means of FEM simulations [8].

Heaters and temperature sensors in the electrode housing will test the coupling of the test mass motion against temperature dependent effects as radiation pressure, radiometer effect and outgassing. Experiments on ground set the coupling factor related to this effects to be of the order $\simeq$100 pN/K in a torsion pendulum experiment [9].

The optical window is an interface which seals the vacuum enclosure containing the electrode housing and, at the same time, lets the laser beam go through for interferometric metrology with the test mass. The optical window is the only non-bonded optical element in the optical metrology subsystem and, since it is clamped in a titanium flange, it will be sensitive to thermal and stress fluctuations. Experiments on ground have allowed modelling the response of the interferometer phase when a heat pulse is applied to the window. The analysis showed that the response can be described by an ARMA(2,1) transfer function relating temperature and phase [10]:

$$G(\alpha_0, \alpha_1, \beta_1) = \frac{\alpha_0 + \alpha_1\, z^{-1}}{1 + \beta_1\, z^{-1}} \tag{2}$$

The model parameters were found to be related with the mechanical (Young modulus) and thermal properties (thermal expansion) of the materials forming the window.

## 3. Closed loop analysis of thermal disturbances

The LTP dynamics control loop is shown in figure 1. The scheme shows two control loops for the two measurement channels: the distance from the first test mass to the spacecraft ($x_1$) and the distance between the two test masses ($x_{12}$). Following the notation in [11], we can describe the dynamics of the two measurement channels in terms of the following set of equations

$$\mathbf{D} \cdot \vec{q} = \vec{g} \tag{3a}$$

$$\vec{g} = -\mathbf{C} \cdot \vec{o} - \vec{g_n} \tag{3b}$$

$$\vec{o} = \mathbf{S} \cdot \vec{q} + \vec{o_n} \tag{3c}$$

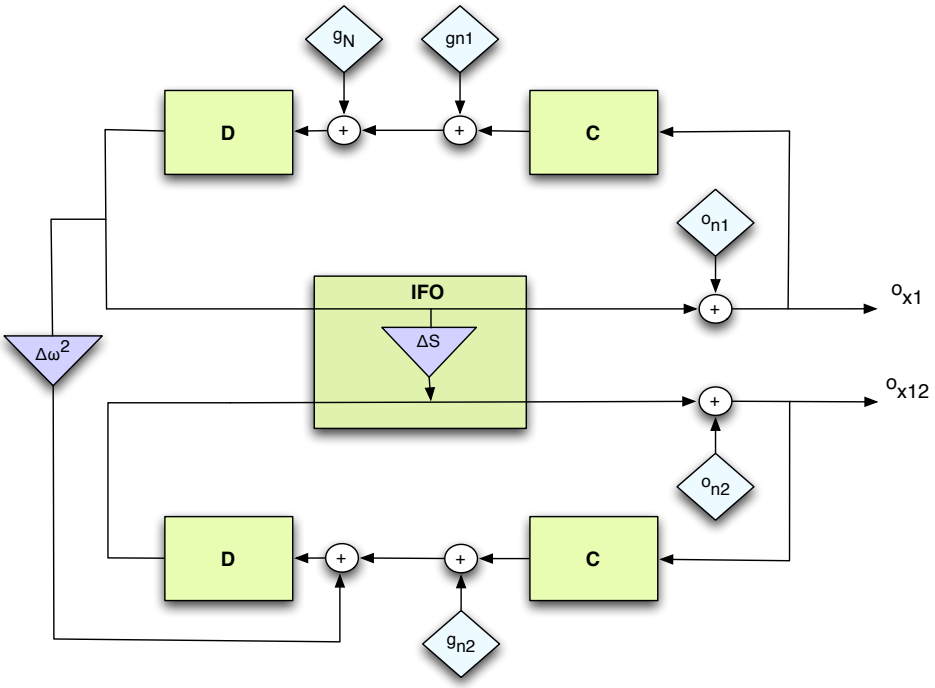


**Figure 1.** Simplified scheme for the dynamics control loop in the LTP. Boxes describe the interferometer (IFO), controllers (C) and dynamics (D). Rhombus represent noise contribution and triangles stand for cross-coupling between first ($o_{x1}$) and second channel ($o_{x12}$).

where the **D** is the dynamical matrix, **C** the controller, and **S** stands for the inteferometer, i.e. the matrix translating the position of the TM, $\vec{q}$, into interferometer read out $\vec{o}$. Subindex $n$ stands for noise quantities, either sensing noise ($\mathrm{o_n}$) or force noise ($\mathrm{g_n}$). These matrices read as

$$\mathbf{D} = \begin{pmatrix} \mathrm{s}^2 + \omega_1^2 & 0 \\ \omega_2^2 - \omega_1^2 & \mathrm{s}^2 + \omega_2^2 \end{pmatrix} \quad \mathbf{C} = \begin{pmatrix} \mathrm{H_{df}} & 0 \\ 0 & \mathrm{H_{sus}} \end{pmatrix} \quad \mathbf{S} = \begin{pmatrix} 1 & 0 \\ \delta\mathrm{S} & 1 \end{pmatrix} \tag{4}$$

where the diagonal terms describes each channel dynamics (e.g. $s^2 + \omega_1^2$ is Newton's law in Laplace domain for the first test mass, being $\omega_1$ the test mass stiffness) and control law (e.g. $\mathrm{H_{df}}$ stands for the drag free transfer function controller on the first test mass). The non-diagonal terms are cross-coupling between the two channels appearing as triangles in figure 1. From the previous expressions we can work out the response of the interferometer once all the dynamical and noise parameters are given,

$$\vec{o} = (\mathbf{D} \cdot \mathbf{S}^{-1} + \mathbf{C})^{-1}(\vec{g}_n + \mathbf{D} \cdot \mathbf{S}^{-1}\vec{o}_n) \tag{5}$$

This equation defines a *nominal output* for the interferometer and this will be the variable that we will use to the effect of thermal forces in the experiment in next section.

### *3.1. Closed loop thermal transfer functions*

In order to evaluate the interferometric response of the experiment to an input signal we need to translate its effect into a measured variable in our previous nomenclature. This effect will differ depending on the heating location under consideration. When heating the electrode housing

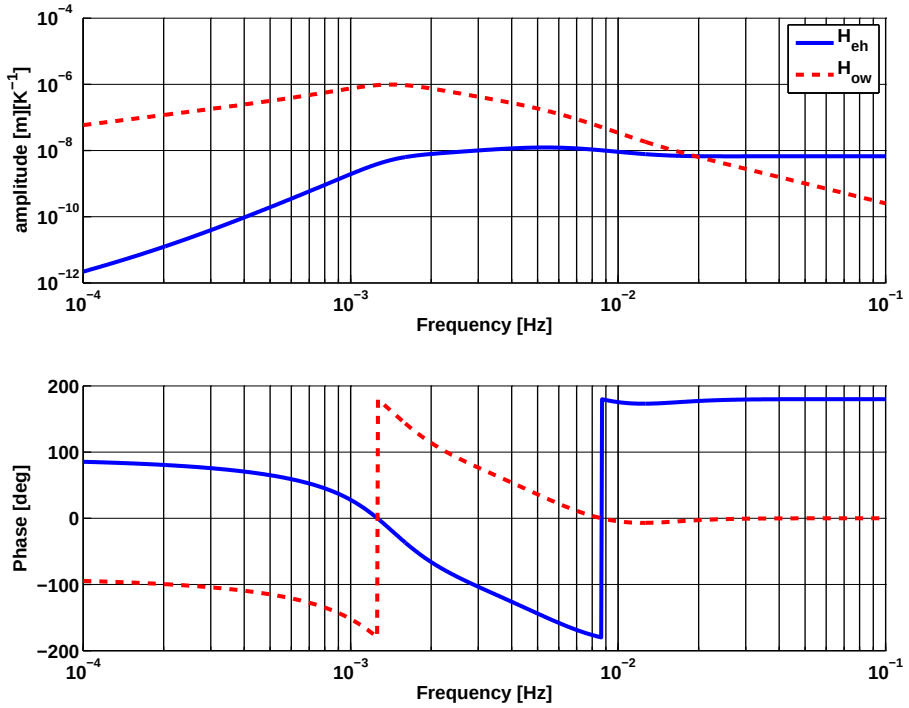


**Figure 2.** Closed loop thermal transfer functions for the electrode housing ($H_{eh}$) and the optical window ($H_{ow}$).

a net force will be applied to the test mass coming from radiation pressure, the radiometer or outgassing effects. Hence we need to introduce a term

$$\vec{g}_{\rm eh} = \mathbf{G}_{\rm eh} \cdot \vec{T}_{\rm eh} \tag{6}$$

in equation (3b), where $\mathbf{G}_{\rm eh}$ is a matrix with the thermal coupling factors and $T_{\rm eh}$ refers to the temperatures measured in the electrode housing. Following the same scheme, a thermal gradient in the optical window will produce a fake test mass displacement, i.e the interferometer will measure a displacement of the test mass though it will not be caused by any displacement but from mechanical stress and thermal distortions on the optical window glass [10]. The coupling in this case is described as a term

$$\vec{q}_{\rm ow} = \mathbf{G}_{\rm ow} \cdot \vec{T}_{\rm ow} \tag{7}$$

in equation (3c). Introducing thermal contributions into the dynamics equation and working out the expressions we end with one equation gathering all the relevant information,

$$\vec{o} = (\mathbf{D} \cdot \mathbf{S^{-1}} + \mathbf{C})^{-1}(\vec{g}_{\rm n} + \vec{g}_{\rm eh} + \mathbf{D} \cdot \vec{q}_{\rm ow} + \mathbf{D} \cdot \mathbf{S^{-1}} \cdot \vec{o_{\rm n}}) \tag{8}$$

from where we derive two closed loop transfer functions for heat inputs coming from the electrode housing or the optical window to the output interferometer read-out,

$$\mathbf{H}_{\rm eh} = (\mathbf{D} \cdot \mathbf{S^{-1}} + \mathbf{C})^{-1} \cdot \mathbf{G}_{\rm eh} \tag{9}$$

$$\mathbf{H}_{\rm ow} = (\mathbf{D} \cdot \mathbf{S^{-1}} + \mathbf{C})^{-1} \cdot \mathbf{D} \cdot \mathbf{G}_{\rm ow} \tag{10}$$

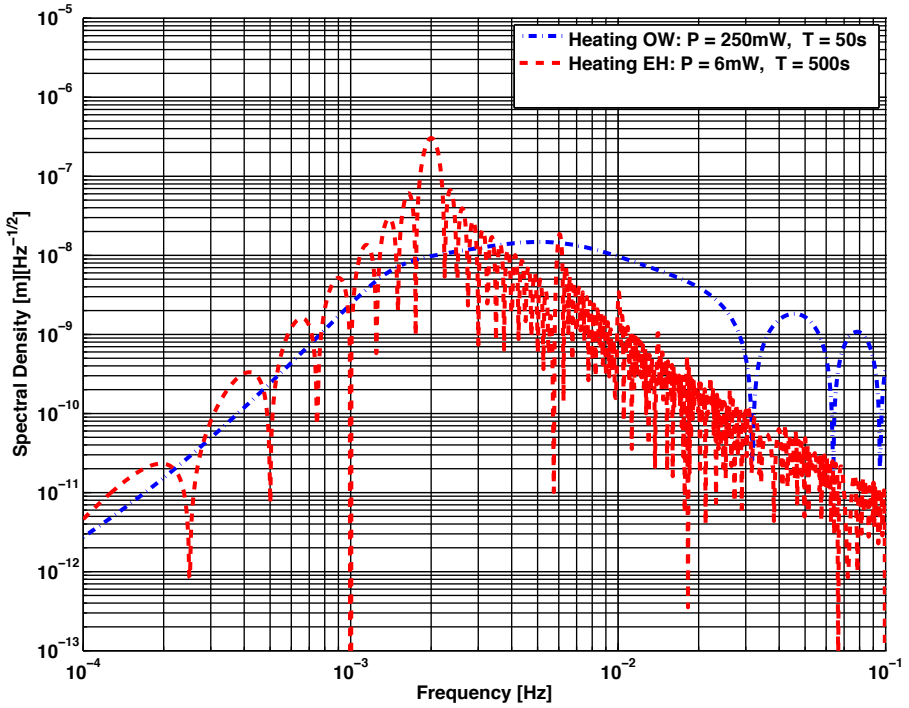


**Figure 3.** Typical thermal signal spectrum. Dot-dashed line represents a 50 s pulse at 250 mW applied to the optical window whereas dashed line is obtained by applying a series of 500 s pulses at 6 mW alternatively to both electrode housing walls to produce a 2 mHz signal.

These expression, evaluated with typical dynamical parameters in figure 2, will help to correctly design thermal experiments in flight. We next show how, according to the derived expressions, the heaters that form part of the thermal diagnostic subsystem can produce a signal clear enough to evaluate the thermal model parameters.

*3.2. Thermal experiments*

The evaluation of the interferometer output during thermal experiments requires the definition of an input thermal signal according to the available hardware in each location. In the electrode housing case, since heaters must be inside the GRS vacuum enclosure and strong vacuum restrictions applies, NTC sensors will be used as heaters and consequently the available power will be only of 90 mW. The heating strategy in this location is to alternatively switch on and off heaters on each side of the test mass in order to apply a periodic force in the test mass so that it peaks in the measuring bandwidth. As seen figure 3 and assuming that the expected in-loop noise floor in the second interferometer channel is $S_{o12}^{1/2}(\omega) \simeq 10^{-10}\,\mathrm{m}/\sqrt{\mathrm{Hz}}$ at 1 mHz, the high sensitivity of the test mass to electrode housing thermal gradients makes it possible to measure this effect with a signal-to-noise ratio high enough to measure the model parameters with high accuracy.

In the optical window case, the available power for the heaters is of 1 W. As before, when compared with the expected instrument noise level, a typical input in this case produces an output strong enough to allow a good parameter estimation.

## 4. Conclusions

The thermal diagnostic subsytem on board the LTP will play a key role in understanding the noise model and to optimise the performace of the experiment. Here we have described the thermal diagnostic subsystem in closed loop, taking into account different noise contributions and the dynamics of the test masses. We have applied this formalism to the electrode housing and the optical window case, and obtained the transfer functions relating a thermal signal input to the measured interferometer signal. These transfer functions will allow a precise definition of the input signal that must optimise the measured output.

According to the current design, we have shown that typical thermal signals applied by the heaters on board the LTP will allow the determination of the parameters describing thermal effects with a good accuracy. The detailed analysis of these signals and the related parameters estimation is ongoing work and will be reported elsewhere.

## Acknowledgments

We gratefully acknowledge support by Deutsches Zentrum für Luft- und Raumfahrt (DLR) (references 50 OQ 0501 and 50 OQ 0601) and financial support from the Spanish Ministry of Education, contracts ESP2004-01647 and ESP2007-61712. JS acknowledges a grant from MEC, and MN a Beatriu de Pinós grant from Generalitat de Catalunya.

## References

[1] Anza S *et al* 2005 The LTP Experiment on the LISA Pathfinder Mission *Class. Quantum Grav.* **22** S125-38
[2] Bender P *et al* 2000, Laser Interferometer Space Antenna: A Cornerstone Mission for the observation of Gravitational Waves, ESA Report no. ESA-SCI(2000)11
[3] Heinzel G *et al* 2004 The LTP interferometer and phasemeter *Class. Quantum Grav.* **21** S581-88
[4] Dolesi R *et al* 2003 Gravitational sensor for LISA and its technology demonstration mission *Class. Quantum Grav.* **20** S99-108
[5] Lobo A *et al* 2003 In-flight Diagnostics in LISA Pathfinder *AIP Conf. Proc.* **873** 522-28
[6] Sanjuan J *et al* 2007 Thermal diagnostics front-end electronics for LISA Pathfinder *Rev. Sci. Instrum.* **78** 104904
[7] Lobo S *et al* 2006 On-ground tests of the LISA Pathfinder thermal diagnostic system *Class. Quantum Grav.* **23** 5177-193
[8] Brandt N *et al* 2005 LISA Pathfinder E2E performance simulation: optical and self-gravity stability analysis *Class. Quantum Grav.* **22** S493-99
[9] Carbone L *et al* 2007 Thermal gradient-induced forces on geodesic reference masses for LISA *Phys. Rev. D* **76** 102003
[10] Nofrarias M *et al* 2007 Thermal diagnostics of the Optical Window on board LISA Pathfinder *Class. Quantum Grav.* **24** 5103-121
[11] Vitale S *et al* 2007 Measurement of LTP dynamical coefficients by system identification, S2-UTN-TN-3045 v1.1, LTP Technical note.